Journal of Materials Processing Tech. 257 (2018) 148–154

Contents lists available at ScienceDirect

Journal of Materials Processing Tech.

journal homepage: www.elsevier.com/locate/jmatprotec

# Joining of aluminum alloy and polymer via friction stir lap welding

Yongxian Huang[a,*], Xiangchen Meng[a], Yuhua Wang[b], Yuming Xie[a], Li Zhou[a]

[a] State Key Laboratory of Advanced Welding and Joining, Harbin Institute of Technology, Harbin 150001, PR China
[b] National Engineering and Research Center for Commercial Aircraft Manufacturing, Commercial Aircraft Corporation of China, Ltd., Shanghai 200436, PR China

ARTICLE INFO

*Keywords:*
Friction stir lap welding
Metal and polymer
Interface characteristic
Microstructure
Tensile properties

ABSTRACT

Sound hybrid joint was achieved with a sufficient mixture of 6061-T6 aluminum (Al) alloy and polyether ether ketone (PEEK) via friction stir lap welding (FSLW) by a tapered thread pin with the triple facets. The larger length ratio between the Al anchor and the rotating pin reached approximately 0.8 at low welding speeds due to the dynamic flow induced by the triple facets. The mechanical interlocking and adhesive bonding attributed to the high-quality joining. Increasing welding speed resulted in the reduction of the adhesion area and the decrease in the size of the Al anchor, deteriorating the mechanical interlocking. A high-quality with the maximum shear bond strength of 20 MPa was achieved through the big Al anchor with a high hardness value. The tapered thread pin with the triple facets has feasible and potential to FSLW of metal and polymer in terms of enhancing mechanical interlocking.

## 1. Introduction

Adhesive bonding and mechanical joining are the main joining techniques between metal and polymer. The adhesive bonding imposes a high difference of surface free energy between metal and polymer. Meanwhile, the adhesive bonding joint is susceptible to temperature or other environmental conditions, described by Amancio-Filho and dos Santos, 2009. Huang et al. (2018a,b) stated that the mechanical joining presents a high susceptibility to stress concentration, and a bonding part, such as screw bolt or rivet, is detrimental to light weight.

Welding techniques, such as ultrasonic welding, laser welding, friction lap welding (FLW) and friction stir lap welding (FSLW) as well as friction spot joining (FSpJ) derived from friction stir welding (FSW), have attracted extensive attentions. Balle et al. (2009) performed ultrasonic welding between 5754 aluminum (Al) alloy and carbon fiber-reinforced polyamide, and consequently the shear strength of 32 MPa was achieved. However, ultrasonic welding is limited to the thin sheets (less than 1 mm) and short joint length. Jung et al. (2016) carried out laser welding of acrylonitrile butadiene styrene (ABS) and zinc-coated steel, and stated that the physical and chemical bonding between a reacted carbon layer and zinc oxide layer were attained. However, bubbles easily generated in the molten polymer near the joining interface, and further deteriorated mechanical properties. Goushegir et al. (2016) obtained a superior shear strength via FSpJ higher than the adhesive bonding.

FLW or FSLW has the huge potential to fabricate metal/polymer hybrid structures. The welding tool of FLW only has a rotating shoulder but without a rotating pin. Liu et al. (2014) utilized FLW to join monomer casting nylon (MC Nylon-6) to 6061-T6 Al alloy sheets. Nagatsuka et al. (2015) join carbon fiber-reinforced thermoplastic to 5052 Al alloy by FLW and stated that a promising joining was attained via MgO layer. Welding parameters played great influence on shear strength of FLW joint (5–8 MPa) due to the adhesive bonding between metal and polymer. However, the bubbles at the interface between metal and polymer significantly reduce the area of load bearing and then deteriorate mechanical properties. Ratanathavorn and Melander, (2015) used FSLW, whose welding tool consisted of a special-designed pin and shoulder, to join 6111 Al alloy and polyphenylene sulphide (PPS). The joining was accomplished through a mixed region containing the surface macro/micro-mechanical interlocking and the adhesive joining as well as the direct partial fiber attachment on the metal sheet. Aghajani Derazkola et al. (2018) also stated that the bonding mechanism of the metal/polymer hybrid structures was mechanical interlocking. Therefore, how to promote mechanical interlocking and then improve joint quality is the key. Welding tool is the core of FSLW, especially the rotating pin which influences material flow and peak temperature. Panneerselvam and Lenin, (2012) reported that a smooth taper pin was detrimental to joint formation under all chosen welding parameters, while a high-quality joint with good formation was obtained by a taper screwed pin for FSW of polypropylene (PP). Payganeh et al. (2011) discussed that a triangle pin with screwed thread owned the sufficient contacting area with welded workpieces, which generated the higher frictional heat and more sufficient material mixture, and consequently obtained good joint formation.

* Corresponding author.
*E-mail addresses:* yxhuang@hit.edu.cn, cn_hyx@163.com (Y. Huang).

https://doi.org/10.1016/j.jmatprotec.2018.02.043
Received 24 October 2017; Received in revised form 26 February 2018; Accepted 27 February 2018
Available online 06 March 2018
0924-0136/ © 2018 Elsevier B.V. All rights reserved.

**Table 1**
Typical material parameters of 6061-T6 Al alloy and PEEK.

| Material | Modulus of elasticity (GPa) | Tensile strength (MPa) | Elongation (%) | Density (g/cm$^3$) | Heat distortion temperature (°C) | Melting point (°C) |
|---|---|---|---|---|---|---|
| 6061-T6 | 70 | 289 | 10 | 2.7 | | 580 |
| PEEK | 2.8 | 97 | 20 | 1.29 | 160 | 334 |

Polyether ether ketone (PEEK) and 6061-T6 Al alloy have become the candidate replacements for application in automotive and aerospace industries in terms of weight reduction. To realize the high-quality FSLW joint and provide technical support for application of FSLW in joining of metal and thermoplastic, a tapered thread pin with triple facets was introduced and attempted to improve mechanical interlocking and enhance mechanical properties. Dissimilar FSLW of PEEK and 6061-T6 Al alloy were mainly investigated from the viewpoints of joint formation, interface characteristic, microstructural evolution and mechanical properties.

## 2. Experimental procedure

The base materials (BMs) were PEEK sheet with a thickness of 7 mm and 6061-T6 Al alloy sheet with a thickness of 2.5 mm, respectively. The physical and mechanical properties of the two BMs are listed in Table 1, which are all tested by experimental analysis. Schematic of FSLW between metal and polymer is shown in Fig. 1a. The 6061-T6 Al alloy lay at the top to generate more frictional heat and prevent molten polymer overflowing out of joint, and the PEEK located at the bottom. A special-designed rotating tool consisted of a concave shoulder in 14 mm diameter and a tapered thread pin with triple facets was employed, as exhibited in Fig. 1b. The length of the rotating pin was 4.8 mm. Welding speed varied from 30 mm/min to 90 mm/min and the increment was 20 mm/min. A rotating velocity of 900 rpm was constant. The plunge depth of the rotating tool and the tilting angle with respect to Z-axis were 0.2 mm and 2.0°, respectively.

The microstructural and mechanical specimens were cut perpendicular to the welding direction. Three metallographic specimens for each welding speed were prepared and observed by optical microscope (OM) and scanning electron microscope (SEM) with an energy dispersive X-ray spectroscopy (EDS). For the SEM observation, a very thin gold layer was coated. In addition, three shear tensile specimens were prepared for each welding speed to evaluate mechanical properties. A shear tensile test was performed at room temperature under a constant crosshead speed of 1 mm/min. Since shear tensile test result is only reported as a load-displacement curve by a test machine, the joining area should be calculated. However, because the real joining area of the shear tensile specimen is not known, a joint width of 20 mm was determined according to the designed tensile shear specimen, as exhibited in Fig. 2. Therefore, the maximum shear bond force divided by the width of 20 mm was used for the calculation of shear bond strength. As

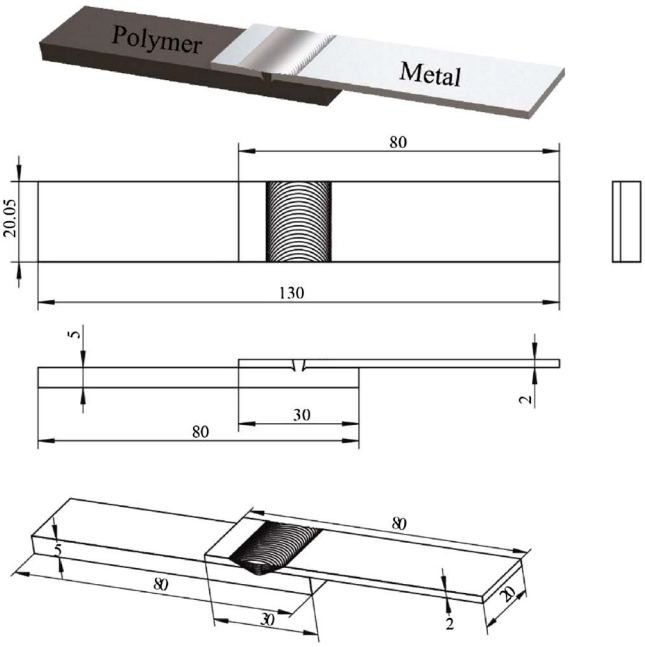


**Fig. 2.** Schematic of the shear tensile specimen (unit: mm).

stated by Khodabakhshi et al. (2014), the Al anchor formed at the hybrid joint and improved the mechanical interlocking, whose hardness controlled the joint strength. The vickers microhardness test was carried out with a load of 50 g and dwell time of 10 s for 6061-T6 Al alloy and a load of 10 g and dwell time of 15 s for PEEK.

## 3. Results and discussion

### 3.1. Joint formation

Fig. 3 exhibits the joint formation in cross section of the hybrid joints using different welding speeds. The joint formation gradually becomes flat with the increase of welding speed. The heat input is relatively higher due to a long dwell and stirring times at a low welding speed of 30 mm/min. During FSW of Al alloys, the welding peak temperature can reach the 70–90% of the melting point of the Al alloys, reported by Rhodes et al. (1997). The sufficient axial force cannot be

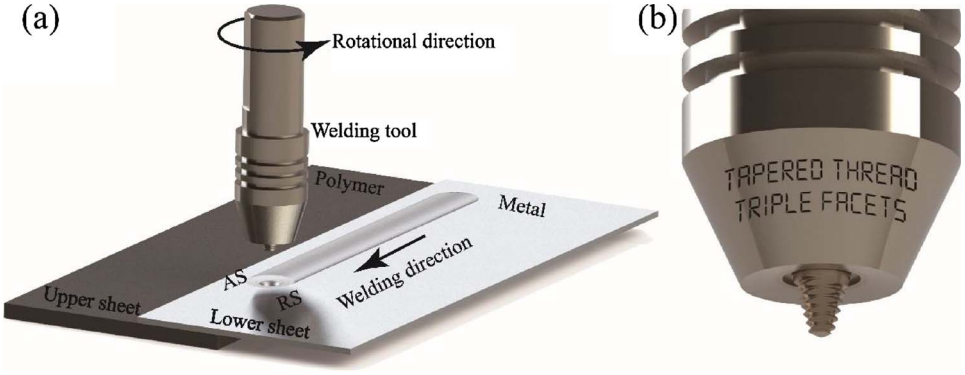


**Fig. 1.** (a) Schematic of FSLW between metal and polymer and (b) rotating tool used in this study.

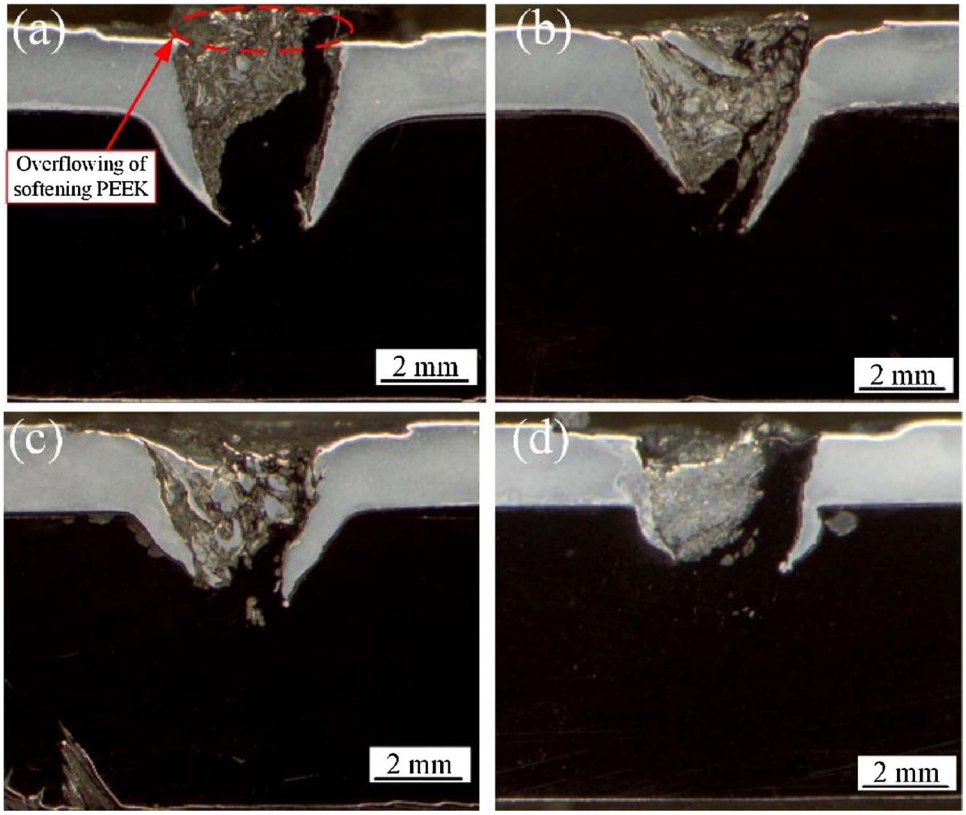


**Fig. 3.** Joint formation in cross section of the hybrid joints: (a) 30 mm/min, (b) 50 mm/min, (c) 70 mm/min and (d) 90 mm/min.

achieved for the displacement controlling machine used in this study since the 6061-T6 Al alloy locates at the top of soft PEEK. Although the peak temperature may slightly reduce, the polymer is still easily softened and then overflows out of the stir zone (SZ), as displayed in Fig. 3a. Moreover, as the rotating shoulder passes the welding region, the mixed materials containing the plasticized metal and soft polymer behind the rotating tool have no obstacle, which easily overflow out of the SZ again because of the big thermal expansion of the PEEK. The overflowing materials of the hybrid joints gradually decrease due to the reduction of heat input increasing welding speed from 50 mm/min to 90 mm/min (Fig. 3b, c and d). Additionally, the width of the SZ for each joint is approximately equivalent to the diameter of the rotating pin. Therefore, the tapered thread pin with triple facets has feasible to join PEEK to 6061-T6 Al alloy sheets under the appropriate process window.

### 3.2. Macro- and microstructures

Fig. 4 displays the partial magnified macrostructures of the hybrid joints at different welding speeds. The PEEK polymer and 6061-T6 Al alloy are broken into small particles or pieces and mixed together under the shear and stirring actions, as indicated in Fig. 4. Besides the SZ, the big Al anchor penetrates into the polymer at the thermo-mechanically affected zone (TMAZ) of advancing side (AS) or retreating side (RS). The formation of the Al anchor is closely correlated with material flow induced by the rotating pin. The rotation of the pin transforms the plasticized Al materials to flow downward along the thread of the left-screwed pin. The Al materials down-bend and penetrate the lap intersection since the polymer is easily softened, and further lead to the formation of Al anchor, as displayed in Fig. 4. The formation of the Al anchor is beneficial to enhancing the mechanical interlocking and then improving tensile properties. The biggest Al anchor of the hybrid joint is achieved at a welding speed of 30 mm/min, which indicates the better mechanical interlocking and larger adhesive bonding area between PEEK and 6061-T6 Al alloy (Fig. 4a). Especially, the Al anchor at the RS is smaller than that at the AS, as displayed in Table 2. This is attributed to that the peak temperature at the AS is higher than that at the RS, and then results in the insufficient soft level of materials in the RS. Moreover, the interface between TMAZ and SZ at the AS indicates a sharp morphology, while the interface between TMAZ and SZ at the RS exhibits an unclear interface, resulting from the differences of the shear stress and material flow at the two sides. It can be postulated that the mechanical interlocking between the plasticized 6061-T6 Al alloy and the re-solidified PEEK polymer at the RS is weaker than that at the AS. Under the thermal cycle and mechanical stirring, the microstructure of the Al anchor is characterized by the bended and deformed morphologies, and the average grain size is approximately 35 μm (Fig. 5b). The microstructures of the metallic chips at the SZ are the same as the Al anchor (Fig. 5c). The sizes of the Al anchors at the AS and RS decrease due to the reduction of heat input when welding speeds reach 50 mm/min and 70 mm/min (Table 2). The length and thickness of the Al anchor sharply decrease with further increasing welding speed to 90 mm/min, which deteriorates tensile properties severely (Table 2). This is because that increasing welding speed decreases the preheat temperature and time on the materials in front of the rotating pin, which results in the insufficient material transfer and then attributes to the reduction of the Al anchor. In Fig. 4a, the surface groove appears at the SZ at a low welding speed. The high welding heat input results in the overflowing of the molten polymer, which causes that the SZ lacks of the filling of the sufficient materials, and then the surface groove defect forms. The defect-free joints are achieved at the other welding speeds, resulting from that no the molten PEEK materials overflow out of the SZ.

Moreover, the length ratio between the Al anchor and the rotating pin is calculated to illustrate the advantage of the tapered thread pin with triple facets, which is compared with the result reported by Shahmiri et al. (2017).

$$\eta = H/L \times 100\% \quad (1)$$

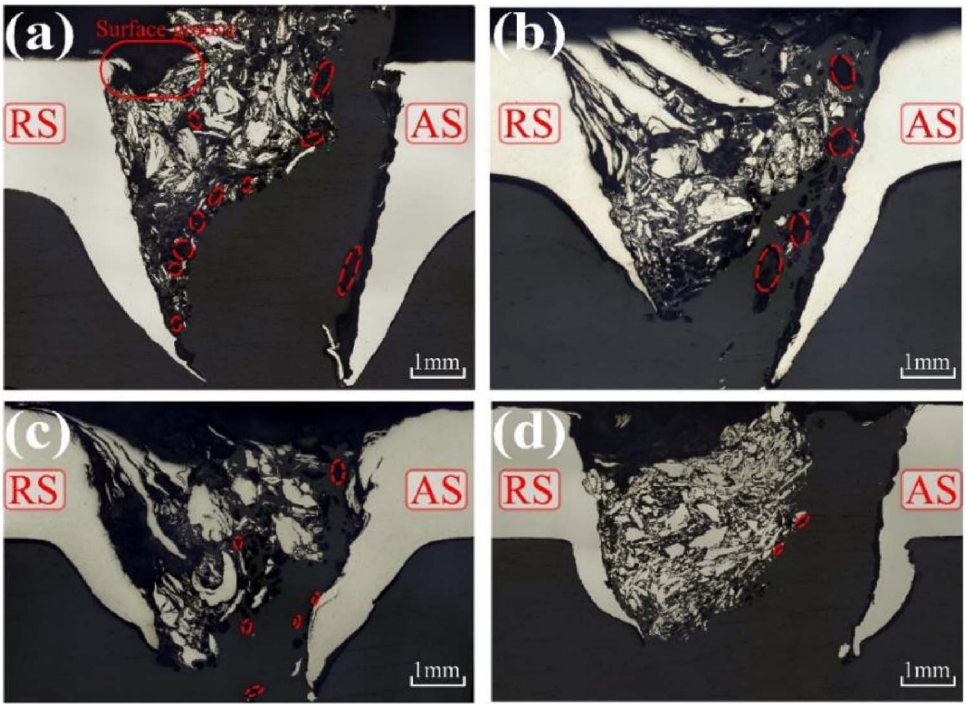


**Fig. 4.** Partial magnified pictures of the macrostructures for the joints at different welding speeds: (a) 30 mm/min, (b) 50 mm/min, (c) 70 mm/min and (d) 90 mm/min.

**Table 2**
Typical characteristics of the Al anchors at the AS and RS of the joints by different welding speeds.

| Welding speed (mm/min) | RS | AS |
|---|---|---|
| 30 | 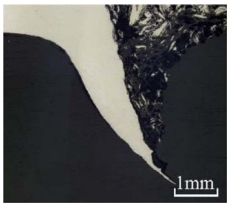 | 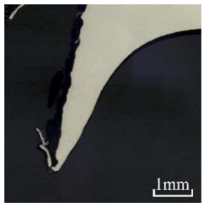 |
| 50 | 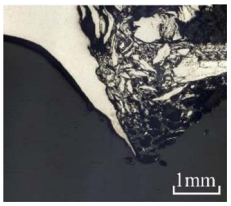 | 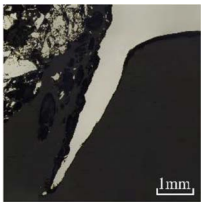 |
| 70 | 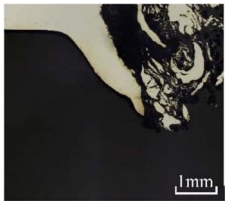 | 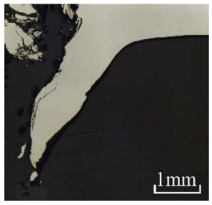 |
| 90 | 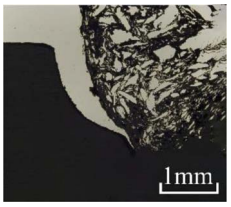 | 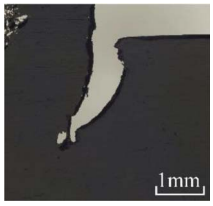 |

Where, $H$ presents the height of the Al anchor whose unit is mm; $L$ indicates the length of the rotating pin. In Fig. 6, the $\eta$ obtained by the tapered thread pin with triple facets at the welding speed of 30 mm/min is higher than that reported by Shahmiri et al. (2017), which means the better material flow happens in this study. Elangovan and Balasubramanian (2008) stated that a square pin produced more pulse/sec (pulses/sec = rotating velocity in per sec × number of flat faces) than a pin without square. The square pin produced 80 Hz and a triangular pin profile produced 60 Hz (pulses per sec) at a rotating velocity of 1200 rpm. Meanwhile, no such pulsating action was observed for a tapered or threaded pin. Moreover, Huang et al. (2018a,b) reported that a pin with triple facets was beneficial to material transfer and then perhaps improving material mixture. Therefore, it is concluded that the tapered thread pin with triple facets can produce more pulsating action and then improve material transfer compared with a thread-tapered pin, which is more suitable for the FSLW between metal and polymer.

Fig. 7 depicts the typical interface between PEEK and 6061-T6 Al alloy. The polymer melts under high peak temperature and then re-solidifies on the surface of metal during cooling stage (Fig. 7a and b), which indicates the occurrence of the adhesive joining between polymer and metal. However, there is a gap appearing at the interface between metal and polymer (Fig. 7b) due to the differences of the coefficient of thermal expansion for PP polymer ($23.8 \times 10^{-6}\,K^{-1}$) and Al alloy ($100–150 \times 10^{-6}\,K^{-1}$). The biggest gap is obtained due to the larger expand with heat and contract with cold induced by higher heat input at a welding speed of 30 mm/min (Fig. 7d). The gap presents the reducing tendency due to the decrease of heat input with the increase of welding speed from 50 mm/min to 90 mm/min. In Fig. 7c, the bubbles appear at the partial interface between metal and polymer, which may be associated with the evolution of structural water, entrapment of air, products of thermal degradation, or differential thermal expansion along the affected volume, stated by Liu et al. (2014). Tan et al. (2015) expounded that the porosities originating from differential thermal expansion presented an irregular and rough inner walls for laser welding joint between carbon fiber-reinforced polymer panels with a polyamide resin (PA6/T) matrix and steel. Meanwhile, the evolution of gaseous products from thermal degradation created the pores with the smooth inner walls. The bubbles easily reduce the area of the load

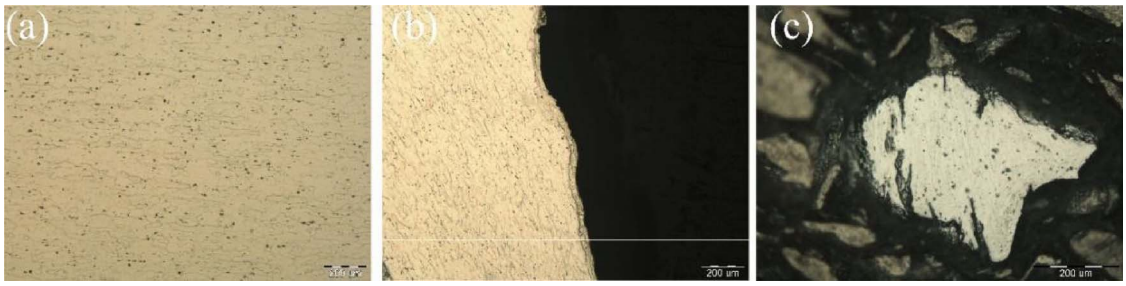


**Fig. 5.** Typical microstructural characteristics of Al alloy at the different positions: (a) BM, (b) Al anchor and (c) Al piece of SZ.

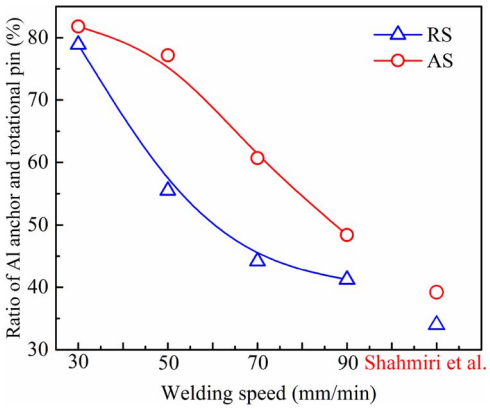


**Fig. 6.** Ratio between the Al anchor and the rotating pin.

bearing and then easily become crack source during shear tensile test, which are detrimental to shear bond properties. In Fig. 4, the number of the bubbles at the interface between re-solidified polymer and metal gradually decreases with the reduction of heat input, which may be beneficial to the improvement of load bearing.

### 3.3. Mechanical properties

#### 3.3.1. Hardness

Fig. 8 exhibits the microhardness distributions at different welding regions. Microhardness of the hybrid joint presents an uneven distribution. The maximum value of 98 Hv is achieved at the BM of 6061-T6 Al alloy. The minimum value of 15.2 Hv appears at the location with the molten and re-solidified PEEK of the SZ. The higher peak temperature and severer plastic deformation induced by the rotating tool during FSLW process are propitious to stirring and mixing the 6061-T6 Al alloy and PEEK together. Meanwhile, the loss of the molecular weight and the reduction of the crystallinity lead to the minimum values at the SZ. Gao et al. (2017) stated that a low crystallinity degree

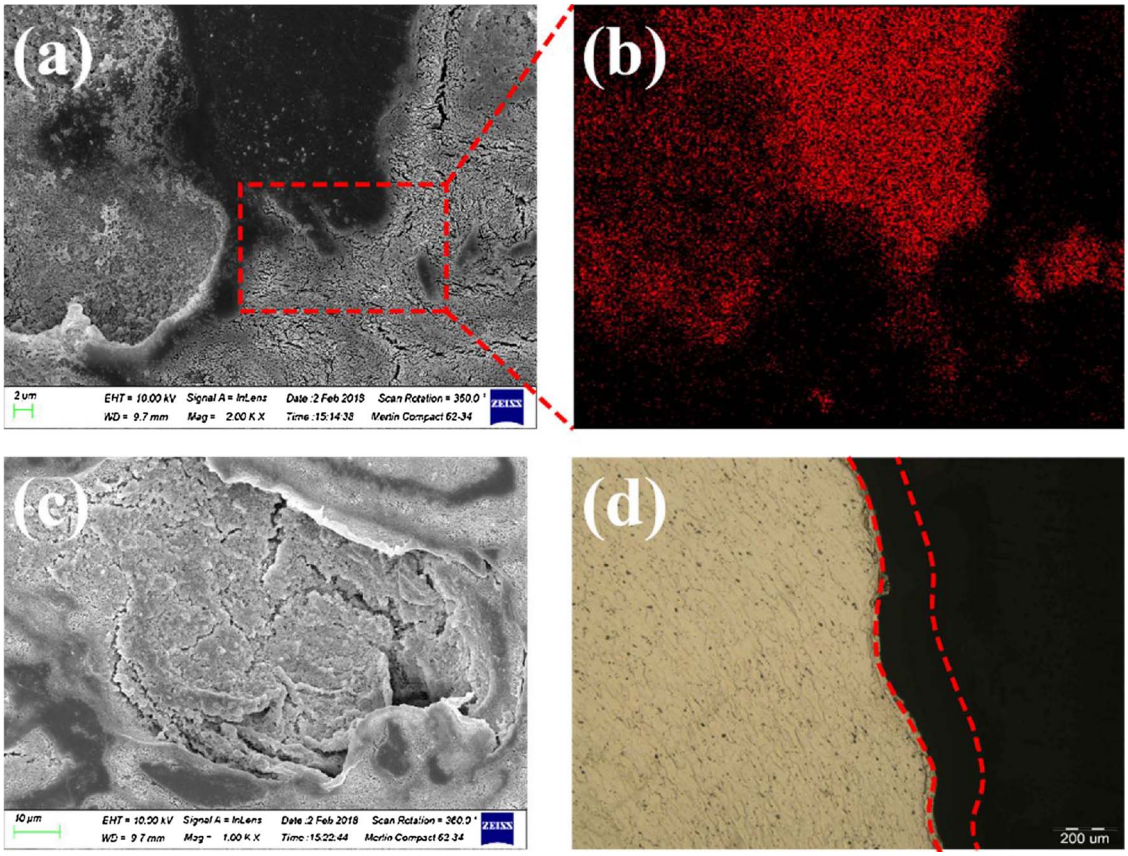


**Fig. 7.** Interface characteristics between polymer and metal in the different regions of the hybrid joint: (a) SEM image, (b) distribution of Al element, (c) bubble and (d) gap near the TMAZ.

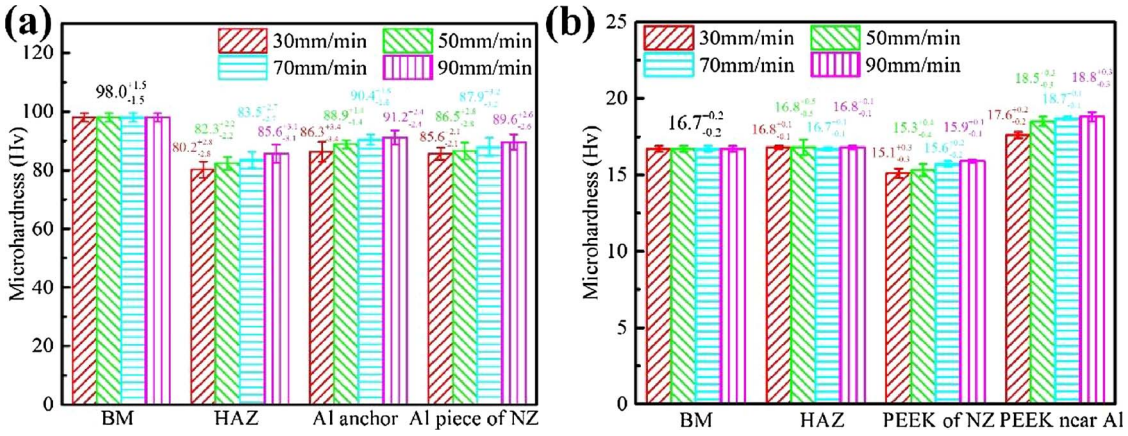


**Fig. 8.** Microhardness distributions of the typical joints: (a) 6061-T6 Al alloy and (b) PEEK.

caused by a high cooling rate was the main reason of the hardness reduction for polymer. Moreover, the average hardness value at the SZ is higher than the BM of PEEK, but lower than BM of 6061-T6 Al alloy due to the presence of the embedded Al pieces or particles in the molten and re-solidified PEEK at the SZ. The Al pieces or particles can act as barrier wall inhibiting the consequent deformation of polymer induced by an indenter, stated by Shahmiri et al. (2017). Therefore, the local hardness near the polymer at the SZ increases. Additionally, different from the HAZ at the side of 6061-T6 Al alloy, the hardness value in the HAZ of the side of PEEK has no obvious variation, resulting from that the PEEK polymer is not affected by welding cycle due to a low thermal conductivity. Strand (2004) also reported that no HAZ was observed for FSW of PP polymer. Importantly, as above-mentioned, the properties of the Al anchor significantly controls the tensile bond properties of the hybrid joint. The hardness value of the Al anchor gradually increases with the increase of welding speed, which may be beneficial to the load bearing of the hybrid joint.

### 3.3.2. Tensile properties

Fig. 9 exhibits the shear bond strength of the hybrid joints at different welding speeds. Shear bond strength is significantly influenced by microstructural evolution caused by welding speed. The shear bond strength firstly increases and then gradually decreases with the increase of welding speed. The maximum shear bond strength of 20.2 MPa is achieved at a welding speed of 50 mm/min. As explained by the microstructural characteristic, because the big Al anchor and the large adhesive bonding area at the interface between metal and re-solidified polymer are obtained, the ability of load bearing is bigger, which is helpful to achieve an excellent joint. Here, the mechanical interlocking attributes to the main joint strength. The sizes of the Al anchors at the welding speeds of 30 mm/min and 50 mm/min are larger, which

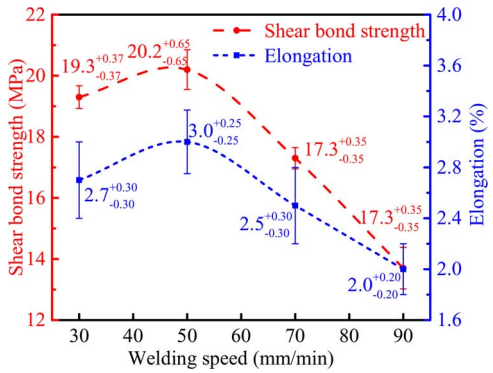


**Fig. 9.** Shear bond strength and elongation of the polymer-metal joints by different welding speeds.

**Table 3**
Maximum shear bond strengths of various polymer-metal hybrid lap joints obtained by different techniques.

| Process | Max. strength (% of polymer strength) | Welding tool | Reference |
|---|---|---|---|
| FLW | 7.8 MPa (10.3%) | A pinless tool | Liu et al. (2014) |
| FLW | 12.9 MPa (9.2%) | A pinless tool | Nagatsuka et al. (2015) |
| FSLW | 5.75 MPa (9.3%) | A cylindrical threaded pin | Ratanathavorn and Melander, (2015) |
| FSLW | 5.1 MPa (16.3%) | A threaded tapered pin | Shahmiri et al. (2017) |
| FSLW | 20 MPa (20.6%) | A tapered thread pin with the triple facets | This study |
| Adhesive bonding | 3.1–13.3 MPa (5–22%) | None | Boone, 2002 |

attribute to the higher shear bond strength. The severe reduction of the Al anchor happens with further increasing welding speed to 90 mm/min. Therefore, the mechanical interlocking induced by the relatively smaller Al anchor is weak or the hardness value of the Al anchor is low for the other three hybrid joints except 50 mm/min, and consequently results in the gradual reduction of shear bond strength. Table 3 lists the shear bond strengths of various polymer/metal hybrid lap joints obtained by different techniques. Under the optimum window in this study, the maximum shear bond strength by the tapered thread pin with the triple facets is higher than those by FLW and FSLW as well as adhesive bonding in naval application. This result indicates that the tapered thread pin with the triple facets has the feasible and potential to replace the adhesive bonding or other welding techniques basing on FSW.

The fracture locations of the typical hybrid joints at the welding speeds of 30 mm/min and 90 mm/min are exhibited in Fig. 10. For all the samples, the fracture locations lie at the interface between metal and the molten and re-solidified polymer at the mechanical interlocking region of AS. As above-mentioned, the gap forms at the interface between the molten and re-solidified polymer, and metal of the hybrid joints at all welding parameters because of the peak temperature and the difference of coefficients of thermal expansion of the two BMs. The crack easily initiates during tensile test, and the nucleation of fracture path forms after this step. With increasing the tensile force, the central crack rapidly propagates along the gap and simultaneously passes through the partial adhesive bonding area between polymer and metal. The final fracture happens when the Al anchor pulls out of the SZ. This conclusion also agrees with the results reported by Shahmiri et al. (2017).

In summary, the critical factors affecting the joint quality mainly

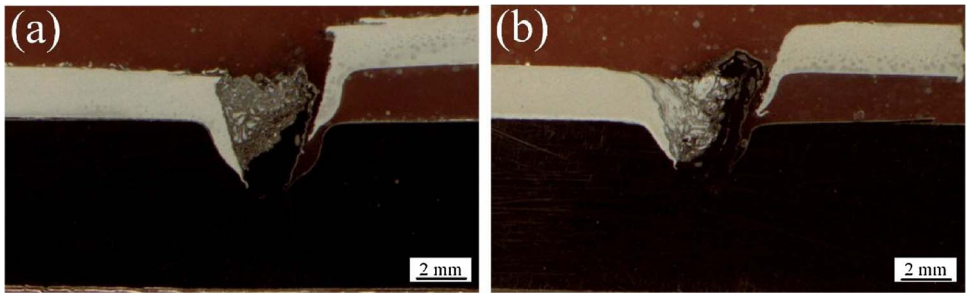


**Fig. 10.** Fracture locations of the hybrid joints: (a) 30 mm/min and (b) 90 mm/min.

contain the Al anchor, crystallization of polymer, gap width of the interface between the molten and re-solidified polymer and metal. The bubbles at the interface between metal and polymer have not been completely avoided. In the future work, how to control these factors and then improve mechanical properties of the hybrid joint is core. Moreover, another key point that is the cyclic loading (fatigue testing) experiment need to be concerned, which has the huge importance in the practical engineering application.

## 4. Conclusions

(1) To promote mechanical interlocking of metal/polymer hybrid joint and further improve mechanical properties, the tapered thread pin with the triple facets was employed to join 6061-T6 Al alloy and PEEK via FSLW. The following conclusions can be extracted.
(2) Feasibility of the tapered thread pin with the triple facets in the FSLW of PEEK and 6061-T6 Al alloy was verified. Sound joint with the strong mechanical interlocking induced by the big Al anchor was achieved.
(3) The Al anchor featured by the bended, deformed and elongated grains penetrated into the molten and re-solidified polymer. Mechanical interlocking induced by the Al anchor attributed to the main joining mechanism. The larger ratio between the Al anchor to the rotating pin was achieved due to the better dynamic flow provided by the tapered thread pin with triple facets.
(4) The decrease of heat input easily reduced the size of the Al anchor and the width of the gap at the interface between the polymer and metal, which is detrimental to the load bearing of joint. The shear bond strength of 20 MPa was achieved at the welding speed of 50 mm/min, which was attributed to the bigger Al anchor and the higher hardness as well as the smaller gap at the interface between the molten and re-solidified polymer and metal.

## Acknowledgement

The work was supported by the Fund of National Engineering and Research Center for Commercial Aircraft Manufacturing (No. COMAC-SFGS-2016-33214).

## References

Amancio-Filho, S., dos Santos, J., 2009. Joining of polymers and polymer-metal hybrid structures: recent developments and trends. Polym. Eng. Sci. 49, 1461–1476.
Aghajani Derazkola, H., Khodabakhshi, F., Simchi, A., 2018. Friction-stir lap-joining of aluminium-magnesium/poly-methyl-methacrylate hybrid structures: thermo-mechanical modelling and experimental feasibility study. Sci. Technol. Weld. Joining 23, 35–49.
Balle, F., Wagner, G., Eifler, D., 2009. Ultrasonic metal welding of aluminium sheets to carbon fibre reinforced thermoplastic composites. Adv. Eng. Mater. 11, 35–39.
Boone, M.J., 2002. Mechanical Testing of Epoxy Adhesives for Naval Applications. University of Maine, Orono, USA, pp. 40–88.
Elangovan, K., Balasubramanian, V., 2008. Influences of tool pin profile and welding speed on the formation of friction stir processing zone in AA2219 aluminium alloy. J. Mater. Process. Tech. 200, 163–175.
Goushegir, S.M., dos Santos, J.F., Amancio-Filho, S.T., 2016. Failure and fracture micromechanisms in metal-composite single lap joints produced by welding-based joining techniques. Compos. Part A-Appl. Sci. 81, 121–128.
Gao, J.C., Shen, Y.F., Li, C., 2017. Fabrication of high-density polyethylene/multiwalled carbon nanotube composites via submerged friction stir processing: evaluation of morphological, mechanical, and thermal behavior. J. Thermoplast. Comp. Mater. 30 (2), 241–254.
Huang, Y.X., Meng, X.C., Xie, Y.M., Wan, L., Lv, Z.L., Cao, J., Feng, J.C., 2018a. Friction stir welding/processing of polymers and polymer matrix composites. Compos. Part A-Appl. Sci. 105, 235–257.
Huang, Y.X., Xie, Y.M., Meng, X.C., Lv, Z.L., Cao, J., 2018b. Numerical design of high depth-to-width ratio friction stir welding. J. Mater. Process. Tech. 252, 233–241.
Jung, D.J., Cheon, J., Na, S.J., 2016. Effect of surface pre-oxidation on laser assisted joining of acrylonitrile butadiene styrene (ABS) and zinc-coated steel. Mater. Des. 99, 1–9.
Khodabakhshi, F., Haghshenas, M., Sahraeinejad, S., Chen, J., Shalchi, B., Li, J., Gerlich, A.P., 2014. Microstructure-property characterization of a friction-stir welded joint between AA5059 aluminum alloy and high density polyethylene. Mater. Charact. 98, 73–82.
Liu, F.C., Liao, J., Nakata, K., 2014. Joining of metal to plastic using friction lap welding. Mater. Des. 54, 236–244.
Nagatsuka, K., Yoshida, S., Tsuchiya, A., Nakata, K., 2015. Direct joining of carbon-fiber–reinforced plastic to an aluminum alloy using friction lap joining. Compos. Part B: Eng. 73, 82–88.
Panneerselvam, K., Lenin, K., 2012. Investigation on effect of tool forces and joint defects during FSW of polypropylene plate. Pro. Eng. 38, 927–3940.
Payganeh, G.H., Dadgar Asl, Y., Ghasemi, F.A., Saeidi Boroujeni, M., 2011. Effects of friction stir welding process parameters on appearance and strength of polyproptlene compsite welds. Int. J. Phy. Sci. 6, 4595–4601.
Ratanathavorn, W., Melander, A., 2015. Dissimilar joining between aluminium alloy (AA 6111) and thermoplastics using friction stir welding. Sci. Technol. Weld. Joining 20, 222–228.
Rhodes, C.G., Mahoney, M.W., Bingel, W.H., Spurling, R.A., Bampton, C.C., 1997. Effects of friction stir welding on microstructure of 7075 aluminum. Scripta Mater. 36 (1), 69–75.
Strand, S.R., 2004. Effects of friction stir welding on polymer microstructure. Brigham Young University.
Shahmiri, H., Movahedi, M., Kokabi, A.H., 2017. Friction stir lap joining of aluminium alloy to polypropylene sheets. Sci. Technol. Weld. Joining 22, 120–126.
Tan, X., Zhang, J., Shan, J., Yang, S., Ren, J., 2005. Characteristics and formation mechanism of porosities in CFRP during laser joining of CFRP and steel. Compos. Part B: Eng. 70, 35–43.